Article

Tunable Silver Nanoparticle Arrays by Hot Embossing and Sputter Deposition for Surface-Enhanced Raman Scattering

Chu-Yu Huang * and **Ming-Shiuan Tsai**

Department of Mechanical Engineering, National Chung Hsing University, Taichung 402, Taiwan;
bsmithqwer1@gmail.com
* Correspondence: tomhuang@nchu.edu.tw

check for updates

Featured Application: The SERS active substrates developed in this study have great potential in areas such as analytical chemistry, biochemistry, and environmental science.

Abstract: Surface-enhanced Raman scattering (SERS) spectroscopy has attracted a lot of attention over the past 30 years. Due to its extreme sensitivity and label-free detection capability, it has shown great potential in areas such as analytical chemistry, biochemistry, and environmental science. However, the major challenge is to manufacture large-scale highly SERS active substrates with high controllability, good reproducibility, and low cost. In this study, we report a novel method to fabricate uniform silver nanoparticle arrays with tunable particle sizes and interparticle gaps. Using hot embossing and sputtering techniques, we were able to batch produce the silver nanoparticle arrays SERS active substrate with consistent quality and low cost. We showed that the proposed SERS active substrate has good uniformity and high reproducibility. Experimental results show that the SERS enhancement factor is affected by silver nanoparticles size and interparticle gaps. Furthermore, the enhancement factor of the SERS signal obtained from Rhodamine 6G (R6G) probe molecules was as high as 1.12×10^7. Therefore, the developed method is very promising for use in many SERS applications.

1. Introduction

Surface-enhanced Raman spectroscopy (SERS) technology has attracted widespread attention since its discovery in 1974 [1]. Comparing to the normal Raman scattering process, SERS is capable of enhancing Raman scattering of analytes by up to a million times or more [2]. It has the potential to provide a very fast and sensitive method of detecting chemicals and biomolecules, which is useful for applications that require fast and highly sensitive detection [3,4]. For example, Caro [5] et al. used a SERS probe for intracellular imaging, SERS signals were strong enough and could be detected even from inside cells. SERS can also be employed to study weak interaction between protein and alizarin [6].

Many SERS substrates use colloidal clusters of noble metal nanoparticles or noble metals with a rough surface to enhance SERS signals. For example, An [7] et al. used silver nanoparticles, tri-iron tetroxide, and carbon cores to form multilayered microsphere particles SERS substrate to detect pentachlorophenol (PCP), diethylhexyl phthalate (DEHP), and trinitrotoluene (TNT). In 2014, Au-Ag-S substrate developed by Cao et al. [8] was used for surface-enhanced Raman detection and photocatalytic degradation of DEHP and DEHA. Liu et al. [9] developed an alloy of gold and silver

nanoparticles urchin shape (hollow Au-Ag alloy nanourchins, HAAA-NUs) as a SERS active substrate to detect 10^{-15} mol/L of DEHP. Most of these studies focus on achieving large enhancement factors, but fail to address the uniformity and reproducibility of these substrates. Due to the random distribution of nanoparticles on the substrate, the interparticle gap size is difficult to control. Therefore, it is difficult to uniformly control the generation of hot spots, resulting in large signal intensity variations, which is detrimental to quantitative analysis. Some researchers have tried to use linker molecules to control the distance between colloidal nanoparticles. For example, Anderson [10] et al. made silver nanoparticle array tethered to a silver film using an appropriate tethering linker such as a dithiol or diamine. However, these linker molecules usually require a dedicated environment (some pH levels or temperatures) to serve the desired purpose, which limits their applications. In addition, linker molecules can block the analyte and prevent it from attaching to the plasmonic surface, which results in a low SERS signal of the analyte. Furthermore, it is possible for the linker molecules to introduce background noise, making the desired SERS signal difficult to measure.

The lack of uniform, reproducible and low-cost SERS active substrates suitable for quantitative analysis remains a major obstacle to the widespread use of SERS for routine analysis [11]. Many research efforts have focused on the development of bottom-up and top-down approaches for the manufacture of controllable and reproducible metal nanostructures for SERS applications [12]. These approaches include: anodic aluminum oxide (AAO) templates assist techniques, lithographic techniques, and oblique angle deposition (OAD) technique. For the metal nanoparticle arrays created using AAO templates, Mu et al. [13] used electroless deposition and adjusted the pH and temperature of the gold plating bath to control the plating rate to achieve the desired particle size and interparticle gap. Lee [14] used densely packed nanowires fabricated from AAO templates. Nevertheless, these approaches require sacrificing the AAO template each time to produce an ordered gold nanoparticle array, which results in increased time and cost expense.

For the lithographic techniques, Sánchez-Iglesias et al. [15] uses block copolymer micellar nanolithography to create seeds for chemical growth of uniform Ag nanoparticle arrays. However, controlling seeds growth at the same rate is not easy, which makes it difficult to obtain a large-sized uniform Ag nanoparticle array. Another disadvantage of lithography is that if standard lithography is used, in order to create a few nanometer gap features, extreme ultraviolet (EUV) will be required, which is very expensive and disadvantageous for low-cost applications.

OAD technology is another method of making SERS active substrates. A number of studies have been conducted to fabricate nanostructured SERS substrates by OAD technology [16,17]. It is a simple method of fabricating SERS substrates, and these fabricated substrates exhibit good sensitivity and uniformity. However, to fabricate SERS substrates by the OAD method, one will need a custom designed electron-beam/sputtering evaporation system. In addition, the vapor incident angle to the substrate normal is around 86°, which means that only a small portion of the material is deposited on the substrate, which results in increased manufacturing costs. Lastly, the anisotropic character of the optical properties, as well as the SERS responses of the substrates [4], lead to the need of special angle coupling of the excitation laser which makes it not convenient to use.

In this study, we used a hot embossing technique to create a uniform and closely packed nanocone arrays on a substrate. Furthermore, by utilizing the self-aggregating nature of nanoscale metal materials, we were able to sputter uniformly distributed silver nanoparticles at the tip of the nanocone array structure. Using this method, we can create a uniform silver nanosphere array with very small gaps between the nanoparticles to create hot spots evenly. We used this structure as our SERS active substrate for rapid detection of low concentrations of analytes. The analytes tested in this study included Rhodamine 6G (R6G) and DEHP. R6G is a highly fluorescent rhodamine family dye, and it is commonly used in SERS experiments as a probe molecule. DEHP is a PVC plasticizer commonly used in food-related containers, such as plastic packaging (PVC cling film), plastic bags, plastic bowls, and plastic cups. According to the Taiwan Ministry of Health, DEHP is defined as an environmental hormone and is defined as a Class 2B carcinogen. The ability to quickly detect low

concentrations of DEHP helps prevent people from eating food contaminated with DEHP, which will benefit people's health.

The developed method can be used to fabricate disposable, low cost and highly sensitive SERS substrates. The results show a strong and uniform SERS enhancement effect. It not only opens up possibilities for using SERS in routine food safety analytics but also helps SERS to be widespread in many other applications as well.

2. Methodology

The method used for the fabrication of silver nanosphere arrays decorated on a polycarbonate substrate with self-organized, hexagonal close-packed nanocone is illustrated schematically in Figure 1. First, a nanocone-shaped groove array structure of aluminum substrate was fabricated by using anodic aluminum self-assembly technique [18–20]. To form a cone-shaped cavity, the anodization and pore widening processes were alternately repeated several times, which creates a top widened and bottom narrow holes, the diameter of these holes are reduced gradually from the top to the bottom of these holes. The fabrication process of the nanocone cavity array of the aluminum substrate including electrolytic polishing, anodic treatment, removal of anodic aluminum oxide. Briefly, a 99.999% purity aluminum substrate was polished in a solution mixed with perchloric acid and anhydrous alcohol in a volume ratio of 1:3.5 and applied with a voltage of 25 V for 2 min. The polished aluminum substrate was anodic oxidation treated in 0.3 M oxalic acid solution with 50 volts for two hours. The anodic aluminum oxide layer was removed by placing the substrate in a 5 wt% phosphoric acid solution at temperature 35 °C for 1 h. The anodization and anodic aluminum oxide removal processes were alternately repeated 5 times to obtain the desired nanocone cavity array structure.
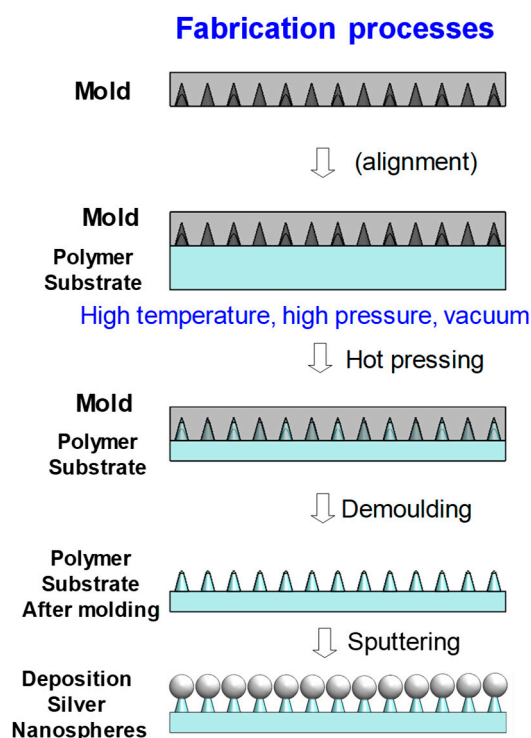
Figure 1. Schematic illustration of the fabrication processes. The nanostructured mold was pressed on a Polycarbonate (pc) plastic substrate using a hot-press molding machine. The nanostructured-nickel mold was heated and pressed on the pc surface for several minutes. After cool down to room temperature, the pc substrate with replicated nanostructure was released from the master mold.

Then a Nickel replica of the nanocone-shaped groove array was obtained by electroforming the nanostructured AAO layer. The nanocone-shaped groove array structured Nickel mold was used as a

master mold. Figure 1. illustrated the hot pressing process. The nanocone-shape groove structured Nickel mold was imprinted on a Polycarbonate(pc) plastic substrate using a hot-press molding machine for heating and pressing the nanostructured nickel mold on pc surface for several minutes. After cool down to room temperature, the pc substrate was released from the master mold. Using this method, we were able to produce many nanocone arrays (moth eye like structure as illustrated in Figure 1) structured pc substrates with low-cost and same quality.

The silver nanoparticles were formed on top of nanocones using sputtering. A dc magnetron sputtering system (Cressington 108 Sputter Coater) was used. Due to the self-aggregating nature of nanoscale metallic materials, the sputtered silver nanoparticles tend to self-aggregate at the tip of the nanocones, and finally form silver nanospheres at the tip of each nanocone (as illustrated in Figure 1). The diameter and interspacing of the nanospheres can be varied by adjusting the sputtering parameters. In order to obtain a uniform and a closely packed array of nanospheres, the appropriate sputtering parameter is needed. In this study, we varied the sputtering duration while the sputtering current and gas pressure were kept at constant (20 mA and 0.02 mbar respectively). The nanostructured polycarbonate substrates were sputtered for different durations to obtain nanospheres with various diameters, and at the same time, the interparticle gaps of the nanospheres were changed accordingly.

3. Experiments

A scanning electron microscope (SEM, JEOL JSM-7800F) was used to examine the surface morphology of the nanocone array and the silver nanosphere array fabricated on the nanocone array. EDS analysis was also performed using the same SEM system. UV–vis absorption spectrum measurements were performed using a HITACHI U3900 spectrophotometer at room temperature in the range of 400–800 nm. The SERS active substrates were placed perpendicular to the light beam to obtain the absorption spectra.

For the SERS studies, the developed surface enhanced Raman scattering sensors were tested using analytes including R6G and DEHP. The developed nanostructured SERS substrates were first immersed in different concentrations of R6G solution and DEHP methanol solution for 12 h, then rinsed with deionized water and dried in air. The SERS spectrometer used was a microscope Raman spectrometer (Tokyo Instruments. Nanofinder 30) with 632.8 nm HeNe laser excitation, and the power of the laser source was set to 0.1 mW. The focused laser spot on the surface of the sample has a diameter of approximately 2 μm and a penetration depth of about 4 μm. The integration time per measurement is 10 s.

4. Results and Discussion

4.1. Characterization of the Developed Substrates

SEM image showed in Figure 2 are the hot imprinted nanocone array on the PC substrate. The spacing between the nanocones is about 130 nm, the width of the nanocone at the base is about 90 nm, and the height of the nanocone is about 140 nm. Silver nanospheres were then deposited by sputtering and the size of these nanospheres was controlled by sputtering duration. Figure 3a–f show SEM images of these silver nanospheres with different sputtering durations of 50, 100, 150, 200, 250 and 300 s, respectively. As can be seen from these figures, the silver nanospheres are uniformly decorated on top of the nanocone array substrate. It can be seen that the longer the duration, the larger the diameter of these nanospheres. However, If the sputtering duration is too long, the nanospheres will start to merge. Figure 3d shows that the diameter of the nanospheres is about 120 nm when the sputtering duration is set to 200 s. This results in a gap between the nanospheres in the range of a few nanometers and is therefore suitable for generating many intense hot spots, which is very helpful for enhancing the SERS effect. Figure 3e,f shows that when the sputtering duration is set to 250 and 300 s, the silver nanospheres start to merge together.

          (**a**)   (**b**)
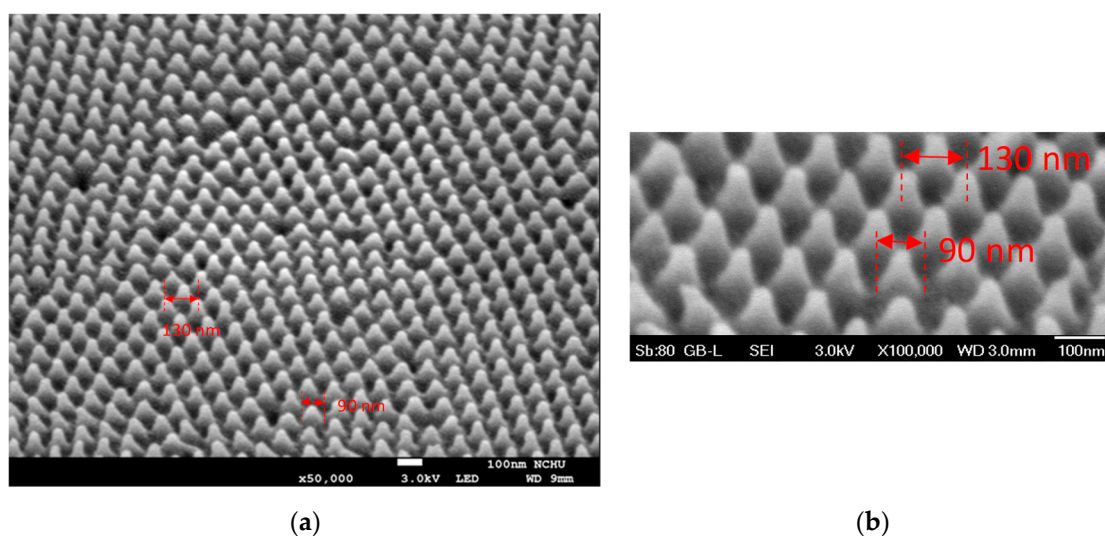
Figure 2. (**a**,**b**) shows the 45 degree view of the hot imprinted nanocone array. (**b**) shows the nanocone image at 100,000× magnification for easier to observe the morphology of nanocone.
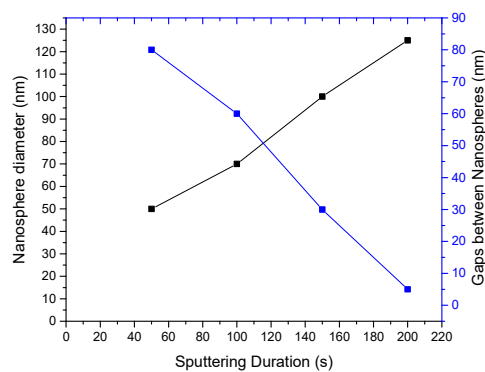
We show in Figure 4 the relationship between the sputtering time and the size of the obtained nanospheres and the gap between the nanospheres. It can be observed that before the nanospheres merge, there is a linear relationship between the size of the nanospheres and the gap them. Therefore, we can adjust the sputtering time accordingly to change the gap size of the nanospheres to optimize the SERS enhancement. After carefully adjusting the sputtering parameters, we were able to make a uniform array of silver nanospheres with a few nanometers interspacing. These uniform and closely packed silver nanospheres can produce a large number of uniformly distributed plasmonic hotspots, which results in high surface enhancement factors and good uniformity. The advantages of this method are that we can prepare a uniform array of nanocones very quickly and at low cost, and the size of the silver nanoparticles can be easily adjusted to change the gap size between them.

EDS was used to analyze the silver nanospheres decorated nanocone array substrate. The EDS spectrum (Figure 5b) shows that the SERS active substrate consisted of 77.5% Ag and 11.48% C. The EDS mapping of Ag of SERS substrate is shown in Figure 5c. From the figure, we can see that the elemental mapping of Ag demonstrates a uniform distribution of the Ag nanosphere on the SERS active substrate.

The UV–vis absorption spectrum was used to analyze the surface plasmon resonance (SPR) characteristics of the proposed SERS active substrates. A series of absorption spectra for the SERS substrate with different sputtering durations (different nanospheres diameters) are shown in Figure 6. As the sputtering duration increase from 100 to 200 s, the diameters of the nanosphere increase from 70 to 125 nm, the absorption peak shifts to the red from 450 to 680 nm. We can observe that the SERS substrate with 200 s sputtering duration shows a broad peak at a wavelength of ~680 nm, and it is closer to the laser excitation wavelength of 632.8 nm. We believe that this absorption peak is caused by the excitation of surface plasmons. Ideally, it would be optimal to use a laser with a wavelength close to 680 nm. The reason we used the 632.8 nm laser is that our Raman system only has a 632.8 nm wavelength laser. If a 680 nm laser is used as the excitation source, it can be expected that the SERS substrate can have a better performance. Comparing these SERS substrates with different sputtering durations, the SERS substrate with a 200 s sputtering duration also showed the highest SERS signal intensity in subsequent experiments (see Figure 7).
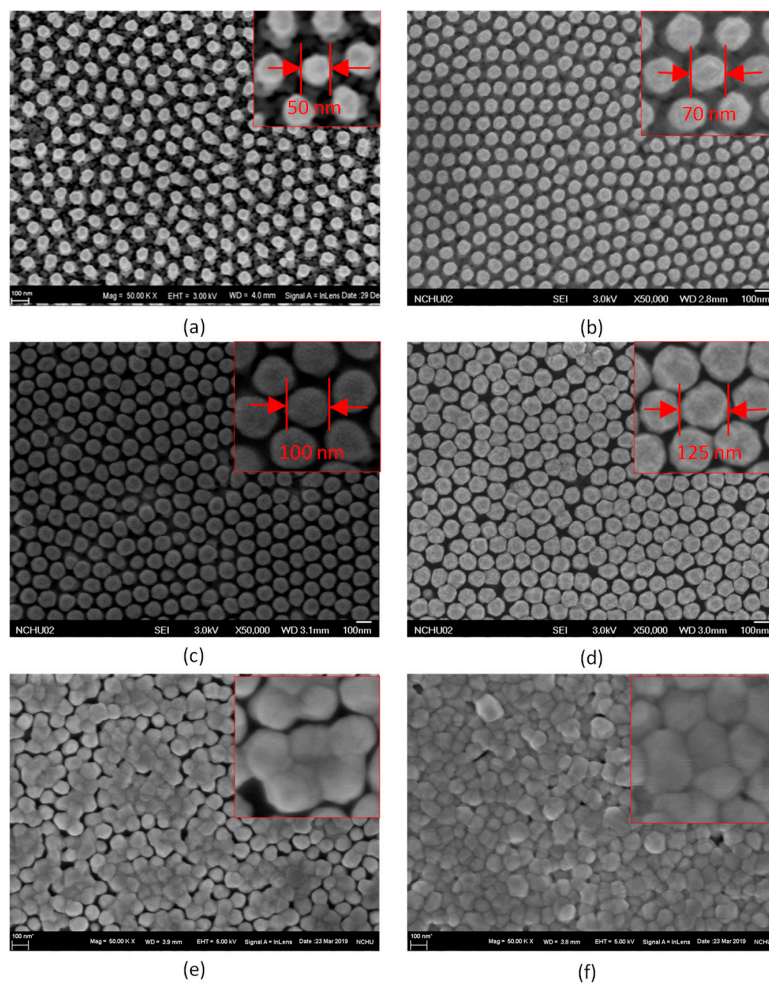
Figure 3. The SEM images show silver nanospheres uniformly distributed on the nanocone array substrate. (**a**–**f**) show different sputtering duration of 50, 100, 150, 200, 250 and 300 s, respectively. Top right corner of each image shows the silver nanospheres at higher magnification for easier to observe their morphology. It can be seen that the longer the duration, the larger the diameter of these nanospheres. If the sputtering duration is too long, the nanospheres will start to merge. By carefully adjusting the sputtering duration, we can fine-tune the diameter of the nanosphere so that we can control the gaps between the nanospheres in the range of a few nanometers.


Figure 4. The relationship between the sputtering duration and the size of the obtained nanospheres and the gaps between the nanospheres.
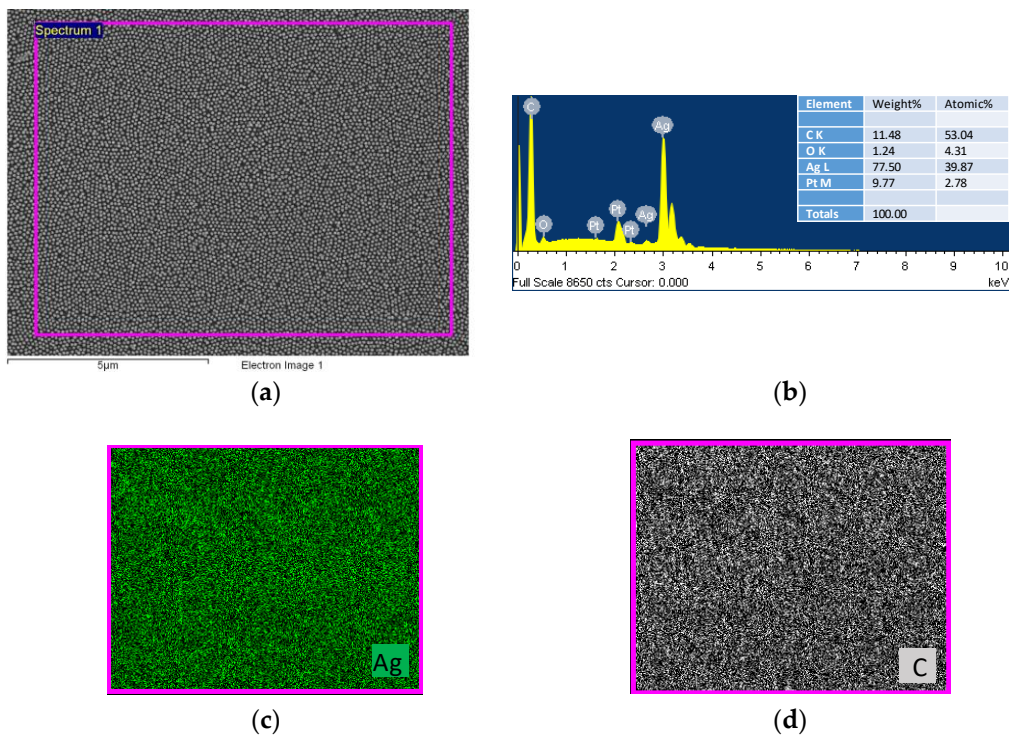
Figure 5. (**a**) Shows the SEM image of the SERS active substrate used for EDS analysis (**b**) Shows the EDS spectrum, it shows that the SERS active substrate consisted of 77.5% Ag and 11.48% C. (**c**) shows the EDS mapping of Ag of the SERS active substrate. (**d**) Shows the EDS mapping of C of the SERS active substrate.
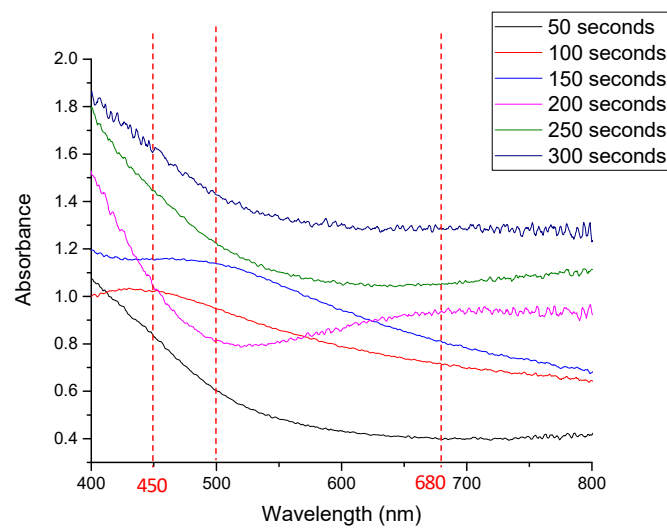

Figure 6. UV-vis absorption spectra of SERS active substrate with different sputtering durations of 50, 100, 150, 200, 250 and 300 s, respectively.
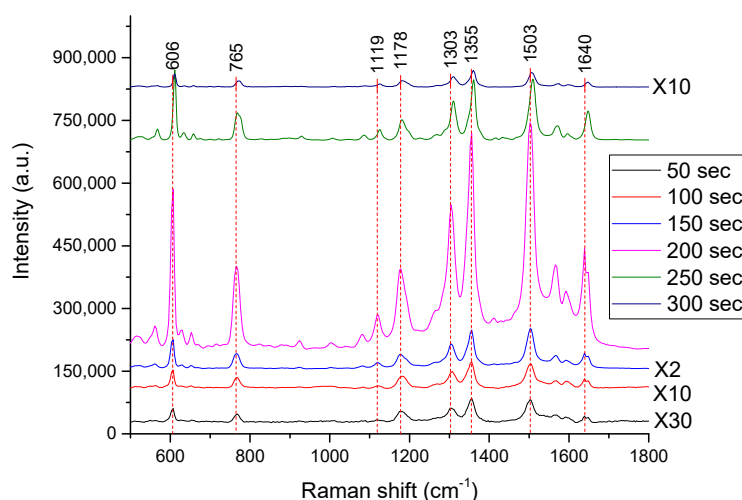
Figure 7. The SERS spectra of the R6G molecules on the developed SERS active substrate with sputtering durations of 50, 100, 150, 200, 250 and 300 s, respectively.

4.2. Performance of the SERS Substrates

In order to see how the different substrate morphologies affect the SERS signal, we measured SERS spectra of R6G solution using substrates with different sputtering times. Figure 7 shows the results of measured SERS spectra of a 10^{-6} M concentration of R6G solution using substrates with different sputtering times. We can see that before the nanospheres merge, as the sputtering duration becomes longer, the gap between the nanospheres becomes smaller and the SERS signal intensity increases rapidly. After the nanospheres merge, the SERS intensity begins to decline. By plotting the peak intensities of 1503 cm^{-1} in the R6G SERS spectra against the corresponding inter-nanosphere gaps, we found that before the nanospheres merge, the intensity of the SERS signal is a logarithmic function of the inter-nanosphere gap, as shown in Figure 8. This result is consistent with the findings of Mu et al. [13]. It also indicates that when the inter-nanosphere gaps are as small as 10 nm or less, we can obtain strong hot spots, so that a good SERS enhancement effect can be obtained.
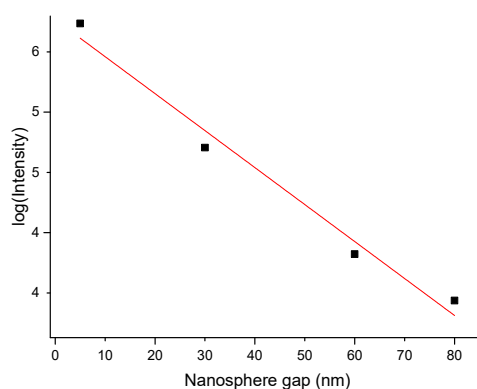

Figure 8. Intensities of the 1503 cm^{-1} SERS signal of R6G recorded as a logarithmic function of the nanosphere gap size.

Figure 9 shows the SERS spectra of blank SERS substrate, bulk R6G, and R6G solutions with concentrations of 1×10^{-6} M, 1×10^{-7} M, 1×10^{-8} M, and 1×10^{-9} M, respectively, using our SERS substrate with sputtering duration of 200 s. The Raman band assignment of the main peaks for R6G were given in Figure 9. Characteristic peaks of R6G at 607, 765, 1176, 1304, 1355, 1503 and 1640 cm^{-1} were clearly observed from these spectra. These spectra demonstrate the good enhancement factor of the SERS substrate we have developed. As can be seen from the figure, the signal from the SERS system itself is very small compared to the SERS signal of the analyte and does not mask the measured

analyte signal. One might question that polycarbonate is a Raman-active compound that can interfere with molecular signals for SERS detection. Here we show that proper decoration of the polycarbonate surface with silver metal can suppress the background Raman signal of the polycarbonate substrate and also prevent melting and degradation of the polycarbonate substrate when exposed to the focused laser beam. This result is consistent with the findings of Geissler et al. [21].
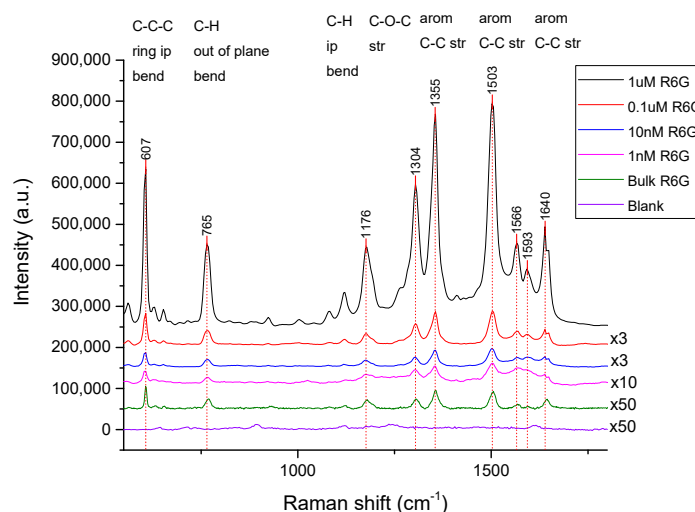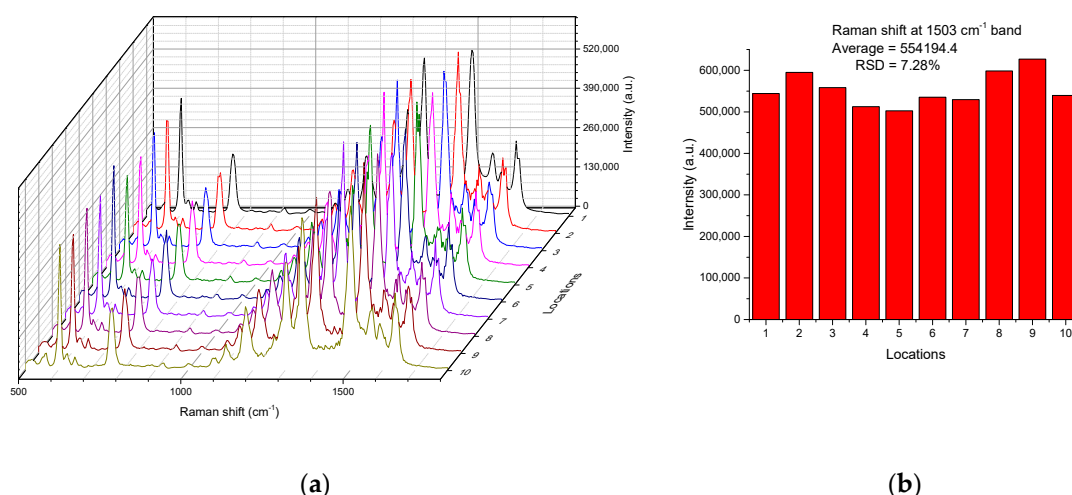

Figure 9. The SERS spectra of blank SERS substrate, bulk R6G, and various concentrations of R6G solution (1×10^{-6} M, 1×10^{-7} M, 1×10^{-8} M, and 1×10^{-9} M, respectively) with our SERS substrates. The Raman band assignment of the main peaks of R6G is given in the figure.

To estimate the enhancement factor (EF) values of R6G, the following commonly used formula [2] was used:

$$EF = (I_{SERS}/I_{bulk})/(N_{bulk}/N_{SERS}) \tag{1}$$

where I_{SERS} and I_{bulk} are the vibration intensity of the SERS and the normal Raman spectra of R6G molecules (the vibration band at 1503 cm^{-1} was selected in this study), respectively. N_{SERS} and N_{bulk} are the number of molecules irradiated by laser spots under SERS and normal Raman of bulk sample condition, respectively. The average surface density of rhodamine 6G (R6G) molecules in densely packed monolayers is reported to be approximately one R6G molecule per 4 nm^2 [22]. Then, the surface coverage of the R6G monolayer on the SERS substrate is 4.15×10^{-11} mol/cm^2 (molecular density = $1/(4 \times 10^{-14})/(6 \times 10^{23})$ mol/cm). For the laser spot of 2 μm in diameter, the N_{SERS} has a value of 1.3×10^{-18} mol ($N_{SERS} = 4.15 \times 10^{-11}$ mol/cm$^2 \times \pi \times 1$ μm^2). For bulk samples, the sample volume is the product of the laser spot area (about 2 μm diameter) and the penetration depth of the focused laser beam (~2 μm). Assuming that the density of the bulk R6G is 0.79 g·cm^{-3}, N_{bulk} can be calculated as 1.04×10^{-14} mol ($N_{bulk} = 0.79$ g·cm$^{-3} \times \pi \times 1$ μm$^2 \times 4$ μm/479.01 g·mol$^{-1} = 2.08 \times 10^{-14}$ mol). For the vibration band at 1503 cm^{-1}, the I_{SERS} and I_{bulk} are 554082 and 791, respectively. Therefore, the EF was calculated to be 1.12×10^7, which is quite high compared to other studies [23,24]. This result is assuming the SERS substrate is densely packed with R6G molecules after immersed in 10^{-6} M R6G solution for 12 h. However, the R6G is likely to cover the substrate at a lower density. Therefore, the SERS enhancement factor calculated here is the lower limits.

In order to calculate the reproducibility of the SERS active substrate, SERS spectra of R6G were obtained at 10 random locations of the SERS substrates with sputtering duration of 200 s. Figure 10a shows the measured spectra from 10 random positions. The SERS intensities of the Raman characteristic peak of the 1503 cm^{-1} band from these locations are further displayed in Figure 10b. The relative standard deviation (RSD) of intensities of the 1503 cm^{-1} Raman characteristic peak was calculated to be 7.28%, which is relatively low compared to other studies [25–27], indicating good uniformity and reproducibility of the fabricated SERS substrates.

(**a**)　　　　　　　　　　　　　　　　　　　　　　　(**b**)

Figure 10. (**a**) The SERS spectra of R6G measured from 10 random positions of the SERS substrate. (**b**) The SERS intensities of the Raman characteristic peak of the 1503 cm^{-1} band from these locations.

The developed SERS substrates were also tested with low concentration DEHP solution. Figure 11 shows measured SERS spectra for DEHP concentrations ranging from 1000 ppm to 2 ppm on SERS substrates. The Raman band assignment of the main peaks for DEHP are given in Figure 11. Raman peaks of DEHP at 1055 and 1433 cm^{-1} are aromatic ring breathing and C=C stretch, respectively. The characteristic peaks of DEHP at 1055, 1433 cm^{-1} are clearly observed from the spectrum. The SERS substrates were found to be able to detect a low concentration (2 ppm) DEHP methanol solution.
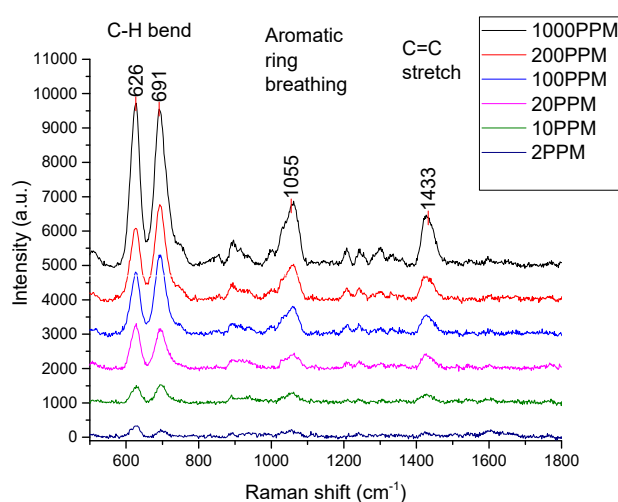
Figure 11. SERS spectra of different concentrations of DEHP (from 1000 ppm to 2 ppm) on the nanostructured SERS substrate. The Raman band assignment of the main peaks of DEHP is given in the figure.

5. Conclusions

In conclusion, we have presented a simple and inexpensive method for synthesizing a uniform nanostructured SERS active substrate with tunable nanosphere diameter and interparticle gaps. The SERS active substrate was fabricated through hot embossing and sputtering deposition. The nanosphere diameter and interparticle gaps were controlled by adjusting the sputtering duration to obtain a uniform and a densely packed silver nanosphere array substrate. According to the SERS experiments, the nanostructured polycarbonate substrate combined with uniformly distributed and closely packed silver nanospheres showed a strong SERS enhancement factor up to 1.12×10^7. The developed SERS substrate has been further applied to the sensitive detection of DEHP molecules

and demonstrated its practical application potential in food contamination detection. Therefore, the developed SERS active substrate is highly promising for use in rapid chemical and biomolecular detection applications.

Author Contributions: Conceptualization, C.-Y.H.; methodology, C.-Y.H.; investigation, M.-S.T.; data curation, M.-S.T.; writing—original draft preparation, C.-Y.H.; writing—review and editing, C.-Y.H.; supervision, C.-Y.H.; project administration, C.-Y.H.; funding acquisition, C.-Y.H.

Conflicts of Interest: The authors declare no conflict of interest.

References

1. Fleischmann, M.; Hendra, P.J.; McQuillan, A.J. Raman spectra of pyridine adsorbed at a silver electrode. *Chem. Phys. Lett.* **1974**, *26*, 163–166. [CrossRef]
2. Le Ru, E.C.; Blackie, E.; Meyer, M.; Etchegoin, P.G. Surface enhanced raman scattering enhancement factors: A comprehensive study. *J. Phys. Chem.* **2007**, *111*, 13794–13803. [CrossRef]
3. Bantz, K.C.; Meyer, A.F.; Wittenberg, N.J.; Im, H.; Kurtuluş, Ö.; Lee, S.H.; Lindquist, N.C.; Oh, S.H.; Haynes, C.L. Recent progress in SERS biosensing. *Phys. Chem. Chem. Phys.* **2011**, *13*, 11551–11567. [CrossRef] [PubMed]
4. Alvarez-Puebla, R.A.; Liz-Marzán, L.M. SERS-Based diagnosis and biodetection. *Small* **2010**, *6*, 604–610. [CrossRef] [PubMed]
5. Caro, C.; Quaresma, P.; Pereira, E.; Franco, J.; Pernia Leal, M.; García-Martín, M.L.; Royo, J.L.; Oliva-Montero, J.M.; Merkling, P.J.; Zaderenko, A.P.; et al. Synthesis and characterization of elongated-shaped silver nanoparticles as a biocompatible anisotropic SERS probe for intracellular imaging: Theoretical modeling and experimental verification. *Nanomaterials* **2019**, *9*, 256. [CrossRef] [PubMed]
6. Cañamares, M.V.; Sevilla, P.; Sanchez-Cortes, S.; Garcia-Ramos, A.V. Surface-enhanced Raman scattering study of the interaction of red dye alizarin with ovalbumin. *Biopolym. Orig. Res. Biomol.* **2006**, *82*, 405–409. [CrossRef]
7. An, Q.; Zhang, P.; Li, J.M.; Ma, W.F.; Guo, J.; Hu, J.; Wang, C.C. Silver-coated magnetite–carbon core–shell microspheres as substrate-enhanced SERS probes for detection of trace persistent organic pollutants. *Nanoscale* **2012**, *4*, 5210–5216. [CrossRef] [PubMed]
8. Cao, Q.; Che, R. Tailoring Au–Ag–S Composite Microstructures in One-Pot for Both SERS Detection and Photocatalytic Degradation of Plasticizers DEHA and DEHP. *ACS Appl. Mater. Interfaces* **2014**, *6*, 7020–7027. [CrossRef] [PubMed]
9. Liu, Z.; Yang, Z.; Peng, B.; Cao, C.; Zhang, C.; You, H.; Xiong, Q.; Li, Z.; Fang, J. Highly Sensitive, Uniform, and Reproducible Surface-Enhanced Raman Spectroscopy from Hollow Au-Ag Alloy Nanourchins. *Adv. Mater.* **2014**, *26*, 2431–2439. [CrossRef]
10. Anderson, D.J.; Moskovits, M. A SERS-Active System Based on Silver Nanoparticles Tethered to a Deposited Silver Film. *J. Phys. Chem. B* **2006**, *110*, 13722–13727. [CrossRef]
11. Cialla, D.; März, A.; Böhme, R.; Theil, F.; Weber, K.; Schmitt, M.; Popp, J. Surface-enhanced Raman spectroscopy (SERS): Progress and trends. *Anal. Bioanal. Chem.* **2012**, *403*, 27–54. [CrossRef] [PubMed]
12. Love, S.A.; Marquis, B.J.; Haynes, C.L. Recent advances in nanomaterial plasmonics: Fundamental studies. *Appl. Spectrosc.* **2008**, *62*, 346A–362A. [CrossRef]
13. Mu, C.; Zhang, J.P.; Xu, D. Au nanoparticle arrays with tunable particle gaps by template-assisted electroless deposition for high performance surface-enhanced Raman scattering. *Nanotechnology* **2010**, *21*, 015604. [CrossRef] [PubMed]
14. Lee, S.J.; Guan, Z.; Xu, H.; Moskovits, M. Surface-Enhanced Raman Spectroscopy and Nanogeometry: The Plasmonic Origin of SERS. *J. Phys. Chem.* **2007**, *111*, 17985–17988. [CrossRef]

15. Sánchez-Iglesias, A.; Aldeanueva-Potel, P.; Ni, W.; Pérez-Juste, J.; Pastoriza-Santos, I.; Alvarez-Puebla, R.A.; Mbenkum, B.N.; Liz-Marzán, L.M. Chemical seeded growth of Ag nanoparticle arrays and their application as reproducible SERS substrates. *Nano Today* **2010**, *5*, 21–27. [CrossRef]

16. Nuntawong, N.; Eiamchai, P.; Wong-ek, B.; Horprathum, M.; Limwichean, K.; Patthanasettakul, V.; Chindaudom, P. Shelf time effect on SERS effectiveness of silver nanorod prepared by OAD technique. *Vacuum* **2013**, *88*, 23–27. [CrossRef]

17. Singh, J.P.; Chu, H.; Abell, J.; Tripp, R.A.; Zhao, Y. Flexible and mechanical strain resistant large area SERS active substrates. *Nanoscale* **2012**, *4*, 3410–3414. [CrossRef] [PubMed]

18. Runge, J.M. *The Metallurgy of Anodizing Aluminum*; Springer International Publishing: Cham, Switzerland, 2018.

19. Brzózka, A.; Szeliga, D.; Kurowska-Tabor, E.; Sulka, G.D. Synthesis of copper nanocone array electrodes and its electrocatalytic properties toward hydrogen peroxide reduction. *Mater. Lett.* **2016**, *174*, 66–70. [CrossRef]

20. Huang, C.Y.; Tsai, M.S. Fabrication of 3D nano-hemispherical cavity array plasmonic substrate for SERS applications. *Int. J. Optomechatron.* **2018**, *12*, 40–52. [CrossRef]

21. Geissler, M.; Li, K.; Cui, B.; Clime, L.; Veres, T. Plastic Substrates for Surface-Enhanced Raman Scattering. *J. Phys. Chem. C* **2009**, *113*, 17296–17300. [CrossRef]

22. Freeman, R.G.; Grabar, K.C.; Allison, K.J.; Bright, R.M.; Davis, J.A.; Guthrie, A.P.; Hommer, M.B.; Jackson, M.A.; Smith, P.C.; Walter, D.G.; et al. Self-Assembled Metal Colloid Monolayers: An Approach to SERS Substrates. *Science* **1995**, *267*, 1629–1632. [CrossRef] [PubMed]

23. Araújo, A.; Caro, C.; Mendes, M.J.; Nunes, D.; Fortunato, E.; Franco, R.; Águas, H.; Martins, R. Highly efficient nanoplasmonic SERS on cardboard packaging substrates. *Nanotechnology* **2014**, *25*, 415202. [CrossRef] [PubMed]

24. Araújo, A.; Pimentel, A.; Oliveira, M.J.; Mendes, M.J.; Franco, R.; Fortunato, E.; Águas, H.; Martins, R. Direct growth of plasmonic nanorod forests on paper substrates for low-cost flexible 3D SERS platforms. *Flex. Print. Electron.* **2017**, *2*, 014001. [CrossRef]

25. Caro, C.; Gámez, F.; Zaderenko, A.P. Preparation of Surface-Enhanced Raman Scattering Substrates Based on Immobilized Silver-Capped Nanoparticles. *J. Spectrosc.* **2018**, *2018*, 1–9. [CrossRef]

26. Wu, W.; Liu, L.; Dai, Z.; Liu, J.; Yang, S.; Zhou, L.; Xiao, X.; Jiang, C.; Roy, V.A. Low-Cost, Disposable, Flexible and Highly Reproducible Screen Printed SERS Substrates for the Detection of Various Chemicals. *Sci. Rep.* **2015**, *5*, 10208. [CrossRef] [PubMed]

27. Sree Satya Bharati, M.; Byram, C.; Soma, V.R. Femtosecond Laser Fabricated Ag@Au and Cu@Au Alloy Nanoparticles for Surface Enhanced Raman Spectroscopy Based Trace Explosives Detection. *Front. Phys.* **2018**, *6*, 28. [CrossRef]